Fracture analysis of one/two-piece clinically failed zirconia dental implants

Fei Zhang[1,2*] Mona Monzavi[3], Maoyin Li[1], Stevan Čokić[2], Al Manesh[4], Hessam Nowzari[3], Jef Vleugels[1], Bart Van Meerbeek[2]

[1] KU Leuven, Department of Materials Engineering, Kasteelpark Arenberg 44, B-3001 Leuven, Belgium.

[2] KU Leuven, Department of Oral Health Sciences, BIOMAT - Biomaterials Research group & UZ Leuven (University Hospitals Leuven), Dentistry, Kapucijnenvoer 7 block a, B-3000 Leuven, Belgium.

[3] Private practice, 1401 N Tustin Ave Suite #345 Santa Ana, Ca 92705, USA

[4] Private Practice, 26800 Crown Valley Pkwy Ste 425, Mission Viejo, CA, 92691, USA

*Email: fei.zhang@kuleuven.be

Conflict interest

No conflict of interest

Abstract

Objectives: Analyzing factors that may have led to fracture of zirconia implants by macro/micro-fractography.

Methods: Six one-piece and ten two-piece full-ceramic zirconia implants from two manufacturers, Z-Systems and CeraRoot, were retrieved after clinical failure. The time-to-failure ranged from 3 to 49 months. Optical and scanning electron microscopy (SEM) were used to analyze the fracture planes at the macro- and microscopic level. Treatment planning, surgical protocol, fracture-origin location and characteristic fracture features were assessed.

Results: The fracture of all implants seemed to have been primarily due to overload in bending mode, while the fracture-initiation sites varied for the one- and two-piece implants. The fracture of all one-piece implants originated in the constriction region between two threads in the endosseous implant part. For two-piece implants, the abutment neck, internal abutment-implant connections and inner threads were found to be the main fracture-initiation sites. Surface defects at the root area for one-piece implants and damages at the abutment surface for two-piece implants were connected to the fracture origins. Importantly, the clinical failures of implants were often found to result from combined effects related to patient aspects, treatment planning/protocols, a high bending moment at the weakest link, implant-surface conditions and specific implant designs.

Significance: This study provided information to be considered for future optimization of treatment planning and the surgical protocol for zirconia implants. Optimization of the surface conditions and the zirconia-starting powder were also suggested.

Keywords: Zirconia implants; Fracture; Fractography; Clinical failure; One-piece; two-piece;

1. Introduction

Ceramic dental implants are increasingly used by dental clinicians and a rising number of companies provide implants with different designs, surface treatments and manufacturing processes [1, 2]. In comparison to other brittle ceramic materials like alumina, zirconia ceramics provide high fracture toughness and bending strength to endure increased interocclusal forces [3]. The osseointegration capacity of zirconia implants is evidenced to be equivalent to that of titanium implants [4-6]. Decreased bacterial biofilm formation and reduced inflammatory cell infiltrate in the peri-implant soft tissue have been reported in favor of implants made of zirconia as compared to titanium [7-9].

The available systematic reviews of zirconia implants reported survival rates of 92-95.6% [10, 11] and the failures have been mainly due to lack of osseointegration or loss of osseointegration following delayed or immediate loading [6, 10, 11]. A fracture rate of 0.2% has been reported for commercially available zirconia implants, which is comparable to existing data on titanium implants [12, 13]. Regardless, long-term randomized controlled clinical results are needed to confirm the currently promising results of zirconia implants and to recommend them as alternative to titanium implants for daily clinical use [11, 14]. Evaluation of clinically fractured implants and experimental investigations have provided evidence that uncontrolled surface treatment such as alumina sandblasting, machining and grinding can lead to surface micro-cracks that may reduce fracture strength and consequently lead to implant fracture [15, 16]. Furthermore, the mechanical properties of zirconia ceramics depend on the manufacturing process including compaction, molding and sintering, and on the powder composition, grain-size distribution and quantity of different grain phases. These factors remain a concern that needs to be studied through *in-vivo* investigations. On the other hand, the knowledge of the clinician on the material properties of ceramic implants and the implementation of a surgical protocol exclusive to such implants is imperative to successful

treatment outcomes. To date, there is no standardized surgical protocol for the placement of ceramic implants and each company has its own set of unique guidelines for the placement of ceramic implants. Considering the major differences in mechanical properties between titanium and zirconia implants, applying a surgical protocol commonly used for titanium implants can lead to complications during and after surgical placement. Therefore, despite the fact that fracture of zirconia implants is a rare event, a precise evaluation of each fracture case *in vivo* can provide valuable data to improve the performance of zirconia implant systems.

Fracture analysis of ceramic dental implants under function necessitates a multidisciplinary methodology, which combines knowledge from clinically related factors with material science and fracture mechanics to allow a better understanding of the reasons behind the failure. Fractography is a valuable technique that provides a precise failure analysis based on interpretation of microscopic fracture-surface characteristics that uncover the direction of crack propagation and the origin of failure [17, 18]. Fractography was first utilized in dental literature to evaluate fracture surfaces of failed ceramic dental restorations with the objective of uncovering the fracture origin [19, 20]. Ever since, it has been increasingly applied for evaluation of *in-vitro* specimens and *in-vivo* ceramic restorations and dental implants [21-23].

In addition, clinical success and fracture analysis of the first-generation monotype one-piece zirconia implants have been reported [15, 22, 24]. A one-piece design avoids multiple components and can be beneficial as it lacks potential stress concentration at the interface and screw attachment. However, the lack of flexibility for detailed adjustments make the clinical indications of one-piece implants challenging for both the surgeon and prosthodontist. In order to answer clinical demands, two-piece zirconia-implant systems have been introduced on the market. Different *in-vitro* assessments and meta-analyses on their fracture resistance are available [25-28]. Long-term clinical data and fracture analyses of retrieved two-piece zirconia implants however are limited. The aim of the present investigation was to combine diagnosis,

4

treatment planning and surgical protocol data with fractography analysis to evaluate the factors that may have led to the fracture of clinically failed one-piece and two-piece zirconia implants.

2. Materials and methods

2.1. Recovered fractured implants

Sixteen clinically failed zirconia implants were recovered from two private practices in California, USA and subjected to fractographic analysis. The time-to-failure varied from 3 to 49 months of intra-oral function. A summary of the investigated implants is provided in Table 1. Implants consisted of monotype (one-piece) and two-piece ceramic implants from two manufacturers, Z-Systems (Oensingen, Switzerland) (n=14) and CeraRoot (Barcelona, Spain) (n=2). All implants were full ceramic implants made of 3 mol% yttria-stabilized zirconia (3Y-TZP) powder. The Z-Systems implants were fabricated using powder pressing, sintering, hot isostatic pressing (HIP), hard machining/grinding, sandblasting with alumina particles and laser modification [29]. There were four first-generation one-piece monotype Z-Systems implants (Z5m), from which one had a tapered design with active threads [Z5m(t)]. Ten Z-systems implants were two-piece implants. Nine out of ten were self-tapping tissue-level implants with cemented abutment (Z5c) and one was a two-piece Z-Systems full-ceramic bone-level implant with screw-retained abutment-implant connection (Z5-BL). The CeraRoot implants were both one-piece implants. The manufacturing process of CeraRoot implants consisted of ceramic injection molding and conventional sintering without further treatment such as HIP. The surface was acid-etched [30, 31].

Regarding the patient-treatment plans, all fractured implants were inserted at a torque of above 50 Ncm. Twelve implants were all inserted in commercially available bone-graft particles that were not in direct contact with the implants. All one-piece Z-systems implants

with a diameter of 4 mm were placed in a molar or premolar site. The surface of the abutment and implant neck of all two-piece Z-Systems implants were ground and re-prepared prior to final impression and crown delivery. The grinding was performed for instance to fix minor angulation-discrepancy errors due to slight off-angle placement of the implant or to reduce the abutment height and so to provide more space in cases with reduced interocclusal space. Grinding with the preparation of minor grooves was in some cases also done to increase surface roughness for better cement retention. Three two-piece Z-Systems Z5c implants failed at the abutment-implant connections near the neck of the implant with portion of the abutment exposed, as shown in Fig. 1a. From the clinical images of the Z-Systems 2p-45m implant shown in Fig. 1a-I, it can also be seen that this two-piece implant was positioned too much above the gingiva, by which the white zirconia implant was visible underneath the crown, having lessened the esthetic outcome. The clinician therefore re-prepared the implant and abutment by grinding the implant and abutment neck in order to get the abutment shoulder at the level of the gum. When conventional (non-digital) impressions are taken for crown fabrication, positioning errors of the height level of a two-piece implant shoulders can be corrected. More details of the clinical treatment planning for each implant are shown in the supplementary Table S1. In particular, one monotype Z5m(t) implant, shown in the supplementary Fig. S1, was placed too deeply in the premolar area in a patient with multiple posterior teeth missing and canine guidance. The bone-level Z-Systems Z5-BL implant, shown in the supplementary Fig. S2, failed at the canine area. The patient presented with canine guidance in laterotrusive movements. One two-piece Z-Systems Z5c implant (Z-Systems 2p-13m) failed at the endosseous portion of the implant. The implant was placed in the lateral incisor area and was positioned too buccally.

Regarding the CeraRoot implants, implantoplasty was performed on the surface of a CeraRoot one-piece implant (CeraRoot 1p-3m) for treatment of peri-implantitis, as shown in

Fig. 1b. Implantoplasty was performed using a rotary instrument equipped with a diamond bur (Henry Schein, Melville NY, USA) to remove the topographic and geometric features (i.e., implant threads) as well as to smoothen the surface. Surface cleaning and disinfection was performed with 0.2% chlorhexidine digluconate. The intraosseous compartment was grafted with an allogenic particulate graft. The graft was compartmentalized with a collagen porcine absorbable membrane. The implant fractured 3 months following implantoplasty. The second CeraRoot case, as shown in Fig. S3, was placed in an entirely grafted bone.

2.2. Fractography analyses

The fractured implants were cleaned in an ultrasonic bath with sodium hypochlorite (5 wt%) followed by pure ethanol. Fracture surfaces were coated with 5-nm thick carbon or platinum. A digital microscope (Tagarno, Horsens, Denmark) was first used to check general fracture patterns, including a compression curl and large twist hackle for the direction of crack propagation (dcp), and to identify the approximate area of the failure origin. Scanning electron microscopy (SEM; FEI-Nova Nanosem 450, FEI, Eindhoven, The Netherlands) was used to analyze the area related to the fracture origin in detail and to characterize the microstructural features at the fracture origin (surface flaws, critical crack sizes, microstructural inclusions as well as intergranular or transgranular fracture modes). In addition, SEM equipped with energy-dispersive spectroscopy (FEI-Nova Nanosem 450) was used to analyze the composition of a dark precipitate observed at the fracture origin of the Z-system 2p-13m implant.

In addition, the available crown surfaces were photographed with the digital microscope and SEM to analyze the occlusal contacts.

3. Results

3.1. Fractography

The general fractographic images taken by light microscopy and the representative fractographic features for the five different fractographic behaviors observed are presented in Fig. 2. Compressive curls are observed on the fracture surface of all 16 recovered implants and the fracture origin was located on the opposite side of the compressive curl. Table 2 classifies the implants into five different cases according to the fracture modes and the implant manufacturer (CASE 1-4 for Z-Systems implants and CASE 5 for CeraRoot implants). More detailed information for each implant is provided in the supplementary document Table S1.

All one-piece implants fractured in the endosseous part in the constriction region between two threads where the cross-section of the implant is the narrowest. The four Z-Systems one-piece implants included Z-Systems 1p-13m/28m/34m and Z-Systems 1p(t)-49m (Fig. 2a, i.e., CASE 1 with corresponding SEM shown in Fig. 3). For two-piece implants, three different fracture-initiation locations were observed: (1) Six two-piece implants, including Z-Systems 2p-3m/16m/28m/29m/30m/32m with a time to failure varying from 3 to 32 months, fractured at the abutment neck (Fig. 2b, i.e., CASE 2 with corresponding SEM shown in Fig. 4). Compared to other conditions, the fracture surfaces appeared rougher with larger twist hackle formed along the abutment's fracture-surface periphery next to the origin, while compressive curls were rather smaller. (2) Three Z-Systems two-piece implants, including Z-Systems 2p-8m/45m and Z-Systems 2pBL-29m, failed at the inner surfaces of the abutment-implant connection or the implant-screw connection (i.e., inner threads) (Fig. 2c, i.e., CASE 3 with corresponding SEM shown in Fig. 5). The abutment was exposed for all three fractured two-piece implants, while the crack-propagation direction was different for each implant. (3) One Z-Systems two-piece implant (Z-Systems, 2p-13m) failed at the implant body (i.e., the endosseous implant part) (Fig. 2d, i.e., CASE 4 with corresponding SEM shown in Fig. 6). The location of this fracture origin was similar to that of the one-piece implant in the constriction

8

region between two threads, where the section of the implant is the narrowest. The failure origin was located below the abutment-implant connection, while the abutment was not exposed.

At last, the two CeraRoot one-piece implants, including CeraRoot 1p-3m/37m (Fig. 2e, i.e., CASE 5 with corresponding SEM shown in Fig. 7), had the same fracture mode as the Z-Systems one-piece implants. They also fractured in the endosseous part in the constriction region between two threads where the cross-section of the implant is the narrowest.

3.2. Z-Systems one-piece implants failed at the endosseous part (CASE 1)

The representative cases for Z-Systems one-piece implants (Z-Systems 1p-13m/28m/34m and Z-System 1p(t)-49m) with (t) standing for tapered are shown in Fig. 3a,b. Irrespective of the parallel-walled (Fig. 3a) or tapered (Fig. 3b) implant designs, all recovered one-piece Z-Systems implants were fractured at the endosseous part between two threads. Laser-modified surface structures characterized by symmetrical parallel grooves were identified at the thread crest and partially at the flanks. The root between two threads, where the fracture originated, was only sandblasted without further laser modification (Fig. 3a-I). A wide v-notch shaped cut was present at the implant surface connected to the fracture origin (Fig. 3a-II,III). The fracture of another type Z-Systems 1p(t)-49m tapered one-piece implant was similar, with a v-shaped deep cut having also been observed at the fracture origin at the implant outer surface between two threads (Fig. 3b).

3.3. Z-Systems two-piece implants failed at the abutment neck (CASE 2)

Representative fracture surfaces of the 6 Z-Systems two-piece implants (Z-Systems 2p 3m/16m/28m/29m/30m/32m) that failed at the abutment neck are presented in Fig. 4, i.e. the case imaged by optical microscopy in Fig. 2b. Grinding/machining grooves along the cylinders

were visible at the abutment surfaces. The fracture origins were connected to the defects found in the grooves. Scars with a ripple pattern (Fig. 4a, Z-Systems 2p-3m) and a v-shaped cut spanning the grooves (Fig. 4b, Z-Systems 2p-28m) were both observed at the fracture origins. Although the grooves were also connected to the fracture origin of the Z-Systems 2P-32m implant, no defect was clearly identified within the grooves at the periphery of the fracture origin (Fig. 4c). This Z-Systems 2p-32m implant was the implant with the longest time to failure amongst this group.

3.4. Z-Systems two-piece implants with failure initiated at the abutment-implant connection (CASE 3)

Fig. 5 shows the fracture surfaces of Z-Systems two-piece implants with fracture initiated at the inner surfaces, more specifically at the abutment-implant connection with angles (cemented implants in Fig. 5a,b) or at the implant-screw connections (i.e. at the internal threads for the screw-retained implant in Fig. 5c). In these three cases, the fracture patterns were complex and the crack-propagation directions were followed/mapped on the fracture surfaces to identify the fracture-initiation sites. For two-piece cemented and self-tapping tissue-level implants (Fig. 5a,b), the fracture-initiation sites involved the internal abutment-implant angles/connections, having resulted in zirconia-abutment exposure. Two fracture-initiation sites were identified for the failure of the Z-Systems 2p-8m implant (Fig. 5a); they were both at the inner connection angles located at the button of the abutment. Similarly for the Z-Systems 2p-45m implant (Fig. 5b), the internal abutment-implant angles were the critical points, but in this case, the angle at the abutment neck was identified as a critical fracture-initiation area as well (marked as origin 1-O1 in Fig. 5b). The fracture of the Z-Systems 2p-45m implant went downwards (for origin 1-O1) or upwards (for origin 2-O2). Regarding the two-piece screw-retained implant (Z-Systems 2pBL-29m), the internal threads were observed to be the weak

fracture-initiation areas. The crack propagation on the Z-Systems 2pBL-29m implant started from the internal threads and propagated horizontally along the implant walls or upward to the implant shoulder. Importantly for all these three cases, no defect was observed at the fracture-initiation sites. Furthermore, no matter how the fractures propagated horizontally or upwards/downwards, they all propagated radially from the internal connections (abutment-implant angles or internal threads) towards outside. Due to the complexity of the crack-propagation paths, some fracture-initiation sites may also not have been identified.

3.5. Z-Systems two-piece implant failed at the endosseous implant part (CASE 4)

One two-piece implant (Z-Systems 2p-13m) failed at the outer surface of the implant body in the constriction region between two external threads of the endosseous implant part (Fig. 6a). The zirconia abutment was not exposed by the fracture. This was the only two-piece implant (out of 10) that failed at the endosseous implant region. A large precipitate of about $10\,\mu m$ with darker contrast was observed at the fracture origin for this two-piece implant fracture. EDS revealed that the precipitate was Al_2O_3, while the matrix region with lighter contrast represented ZrO_2 (Fig. 6b). Similar Al_2O_3 precipitates ($>2\,\mu m$) were also randomly observed at other locations at the fracture surface, although not being the cause of crack initiation.

3.6. CeraRoot one-piece implant failed at the implant endosseous part (CASE 5)

Similar to the Z-Systems one-piece implants, the two CeraRoot one-piece implants all fractured at the endosseous part of the implant, more specifically in the constriction region between two threads. The fracture origin was located at the external surface with hackle radiating from the implant surface in the direction of crack propagation (marked with arrows in Fig. 7). The implant surface of the CeraRoot 1p-3m implant clearly showed many damages/chips (Fig. 7a-

I) from the implantoplasty treatment, as compared to the non-treated CeraRoot 1p-37m implant (Fig. 7b-I). Higher magnification of the CeraRoot 1p-3m implant (Fig. 7a-II) displayed that the fracture origin was connected to the rough surface, while a large chipping defect of ~50 µm in depth was observed at the fracture-origin site. For the CeraRoot 1p-37m implant (Fig. 7b-II), a particular critical flaw was not identified at the site of fracture origin.

3.7. Occlusal contact and anatomical orientation

Fig. 8 shows the anatomical orientation and the surface conditions of the crowns that were placed on the representative implants of the five fracture cases classified in Fig. 2 and Table 2. All crowns were monolithic zirconia crowns. While the surface glaze was often worn out, indications of occlusal contacts were solely observed on the occlusal surfaces of some crowns (Fig. 8a,d,e). These contacts were judged to result from normal fysiological functioning. In addition, the occlusal surfaces of several crowns showed heavy grinding marks (Fig. 8b,c), which probably represent intra-oral crown-surface adjustments carried out by the clinician. Occlusal contacts could hardly be observed in case of heavy grinding. In the case of the Z-Systems 2p-16m implant (Fig. 8b), almost the whole occlusal surface was heavily ground, while no clear evidence of wear facets was found. Similarly, on the crown surface of the Z-Systems 2p-45m implant (Fig. 8c), grinding grooves also covered almost the whole occlusal surface in the mesial-distal-palatal areas. Several small contacts were observed on the mesio- and distobuccal cusps. What is important for this specific Z-Systems 2p-45m implant is that the crown had a large bulky buccal extension, by which the central axis of the implant was off-centered.

3.8. Fracture-surface microstructure of zirconia grains

The fracture patterns of zirconia grains in the Z-Systems and CeraRoot implants consisted of mixed inter- and transgranular fractures (Fig. S4 in the supplementary document). Residual porosities, marked with black arrows in Fig. S4b, were observed in the CeraRoot implants. Nevertheless, these pores were not identified as the critical defects causing failure of the CeraRoot implants. The Z-Systems implants looked denser with pores rarely having been detected. The zirconia grains of the CeraRoot implants were much finer than those of the Z-Systems implants.

4. Discussion

In the present study, 16 fractured full-ceramic zirconia implants were examined with a time-to-failure varying from 3 to 49 months. A compression curl was present at the fracture surfaces of all investigated implants (Fig. 2). This is typical for a flexural fracture, revealing that all studied zirconia implants were primarily loaded in the bending mode [15, 18], independent of implant designs, surface conditions and fracture-origin locations. This agrees with previous fractography reports of various one-piece clinically failed zirconia implants [15, 24]. Similar fractographic features including twist hackle and compression curl were also observed for the two-piece zirconia implants fractured in *in-vitro* load-to-failure experiments [32-34]. Although all implants must have cyclically been loaded in oral environments, arrest lines indicating cyclical loading in flexure were generally not observed from the fracture surfaces of one-piece implants studied in this study. The morphology of fatigue-fracture surfaces in ceramics is generally known to be almost identical to that under monotonic loads [35], whereas arrest lines, which could be visible above the fracture-origin sites, were reported in few clinically placed zirconia implants/restorations [15, 18, 36]. Arrest lines were observed at the fracture surfaces of two-piece implants that had failed at the abutment-implant connection with the abutment

exposed (i.e., CASE 3); these arrest lines were used extensively to map the crack-propagation directions (Fig. 5).

The implant design (one- and two-piece) was shown to have a clear influence on the crack-initiation locations (Table 2). All investigated one-piece implants fractured between two threads at the endosseous part (CASE 1 and CASE 5), with the fracture origin being located at the implant surface. This was independent of the specific implant shape and implant manufacturer, as the parallel-walled one-piece Z-Systems implant (Z5m, Fig. 3a), the tapered one-piece Z-Systems implant (Z5t, Fig. 3b), and the CeraRoot one-piece implants (Fig. 7) all failed at a similar location. The fracture origins of all Z-Systems and CeraRoot one-piece implants were clearly connected to surface flaws found at the constriction region between two threads. This was consistent with previous reports on one-piece implants with different shapes from other manufacturers [15, 16]. The v-shaped surface flaw observed at the fracture origin of the Z-Systems one-piece implants was probably caused by alumina sandblasting (CASE 1, Fig. 3). Although sandblasting and laser modification on Z-Systems implants are performed to promote osseointegration, they could have a significant impact on the zirconia implant's mechanical performance. Sandblasting of dental zirconia can be beneficial for an enhanced tetragonal-to-monoclinic phase transformation and generation of compressive stress [37-39], this depending on the sandblasting protocol (particle size, pressure and distance) [40-43]. The sandblasting-induced flaws and slow crack-growth effect may also countervail the strengthening effect, lowering the reliability [38, 39] and long-term fatigue performance of zirconia [44, 45]. In addition, although laser modification of Z-Systems implants induced columnar grains, tetragonal-to-monoclinic transformation and (micro-)cracks [29, 46], these laser-related surface damages were not involved in the fracture of the Z-Systems implants. This should be ascribed to selective surface modification by the laser. The laser treatment was applied to the thread crest and partially to the flanks (Fig. 3a-I), whereas the critical stress-

14

concentrated root between two threads was not laser-treated. Furthermore, all one-piece Z-Systems implants placed in a molar and pre-molar site had a diameter of 4 mm (Table 1), which is considered narrow for zirconia implants placed in the molar area and is not recommended by the manufacturer. Previous studies demonstrated that the fracture incidence of implants is associated with a decreasing implant diameter [15, 22, 47].

Regarding the fracture cause of the CeraRoot one-piece implants (CASE 5), the surface chipping observed for the CeraRoot 1p-3m implant (Fig. 7a) may have been induced by implantoplasty of the endosseous portion of the implant. In this particular case, implantoplasty was conducted to smoothen the surface of the implant's threads in order to remove the implantitis-related bacterial biofilm [48]. Ideally, one should smoothen sharp edges and reduce surface roughness without causing damage. In the case of the CeraRoot 1p-3m implant, implantoplasty was conducted in an attempt to clean the surface and remove the threads, a procedure widely recommended for Ti implants [49-51]. However, chipping damages were identified at the remaining 'threads'. Although implantoplasty may be a common procedure to treat peri-implantitis around titanium implants [52], its application needs to be re-considered for zirconia implants as it can destabilize the zirconia-surface grains and influence the fracture strength of the zirconia implant [53]. Nevertheless, besides the potential induction of defects by implantoplasty, the early failure at 3 months of the CeraRoot 1p-3m implant following implantoplasty may also be due to heavy bone loss with little bone support left, as can be seen from clinical images in Fig. 1b-II, combined with a high bending moment with stress concentration at the weakest implant link. Regardless of the implant-surface modification (implantoplasty) being performed or not, the survival rate of implants treated for peri-implantitis was reported to be primarily influenced by the amount of bone loss at the time of treatment [54]. Further studies on the effects of implantoplasty of zirconia implants should be conducted.

In terms of two-piece ceramic implants, the abutment neck (Fig. 2b, Fig. 4; CASE 2) and the abutment-implant connection (Fig. 2c, Fig. 5; CASE 3) were critical regions. The majority (6 out of 10) of the studied two-piece implants fractured at the abutment neck (Fig. 2b; CASE 2). All 6 implants and their abutments were ground and re-prepared by the clinician prior to final restoration, this because of different reasons mentioned in the patient-treatment plans (Materials and methods, section 2.1). However, it was not clear which specific part of the abutment was ground and how the grinding/re-preparation was exactly performed by the clinician. Furthermore, the grooves observed at the abutment neck could have originated from the implant-manufacturing process as well. In any case, flaws at the abutment surface were evident and included ripple-shaped grinding scars and v-shaped sharp flaws (Fig. 4a, b). These surface defects were also connected to the fracture origin (Fig. 4a, b). Grinding has generally been reported to reduce not only the strength but also the reliability of zirconia ceramics [38, 39]. Previous *in-vitro* investigations on ceramic implants have also suggested that grinding zirconia implants negatively influences the fracture strength of the implants [55]. V-shaped sharp defects, as observed in Fig. 4b in particular, have been shown to degrade the material's fatigue resistance [56]. Furthermore, in contrast with one-piece implants, the abutment neck is one of the stress-concentration areas [57]. The abutment-surface quality of the two-piece zirconia implant is therefore very critical.

Three fracture cases out of 10 two-piece implants occurred at the inner abutment-implant connection (CASE 3). Microscopically, no critical defect was observed at the fracture-initiation sites at the inner implant surfaces (Fig. 5). A similar failure pattern at the abutment-implant connection without clear defect was reported for other two-piece zirconia implants fractured in *in-vitro* experiments [32]. In another *in-vitro* investigation, implants inserted at torque values ranging from 46 Ncm to 70.5 Ncm all fractured following a pattern similar to that observed in the current investigation; the fracture involved the bottom of the abutment-implant connection,

which had already reached a sub-crestal position [58]. The cause of failure was probably due to the high stress concentration along the abutment-implant connection. Presence of excessive mechanical force from disproportionately large crowns can also lead to failure of implants at the abutment-implant connection. In particular in the case of the Z-Systems 2p-45m implant, since the central axis of the implant was off-centered (Fig. 5b-V) and the contact loading was excentric from the implant's central axis (Fig. 8c), exaggerated bending and stress concentration may have been produced especially at the internal angles at the abutment-implant connection (Fig. 5b).

One single fracture of a two-piece implant (Z-Systems 2p-13m) occurred at the endosseous implant part (Fig. 6; CASE 4). The failure of this implant was probably due to several combined reasons. This implant was installed too buccally and the implant failed from palatal toward buccal (Fig. 8d). The alumina precipitate of ~10 µm noticed in the area between two threads (Fig. 6) could also have contributed to this particular fracture. A small alumina amount of ~0.25 wt% was added to dental zirconia to aid sintering and improve aging resistance [59]. Well-dispersed 0.25 wt% alumina in the starting powder can almost completely be dissolved and is segregated as Al^{3+} at the zirconia-grain boundaries during sintering. Any excess alumina will present as individually dispersed alumina grains in the microstructure [60]. The presence of non-homogeneously dispersed large alumina precipitates in zirconia ceramics is not rare [61]. The particular failure of the Z-Systems 2p-13m implant emphasized the necessity of homogeneously dispersing the alumina addition.

With regard to the different implant-manufacturing processes, as presented by a previous *in-vitro* investigation [44], conventional processing consisting of pressing, sintering and hot isostatic pressing (HIP) gave rise to better densification than injection molding (Fig. S4b). The different microstructures (residual porosities and zirconia-grain size) however were not related to the fracture origins studied in this work.

Conclusion

The crack-initiation locations and implant-fracture causes vary for one- and two-piece zirconia implants, hereby indicating different areas of stress concentration for each system. The clinical failures of implants were found to result from combined effects related to patient aspects (like heavy bone loss at the time of implantoplasty treatment), treatment planning/protocol (like off-centered implant positioning), implant-surface qualities and specific implant designs (two- or one-piece implants). The surface sandblasting at the root area and the starting powder can be optimized. The treatment planning and surgical protocol should also be optimized to ensure long-term success and survival of zirconia implants. Damages induced at the abutment surface for two-piece implants, caused either during the machining-manufacturing process or by grinding and re-preparation by the clinician prior to final restoration, should be avoided. Implantoplasty of ceramic implants in case of heavy bone loss should be re-considered or at least be subjected to further study.

Conflict interest

No conflict of interest

References

[1] Cionca N, Hashim D, Mombelli A. Zirconia dental implants: where are we now, and where are we heading? Periodontol 2000. 2017;73:241-58.
[2] Osman RB, Swain MV. A Critical Review of Dental Implant Materials with an Emphasis on Titanium versus Zirconia. Materials. 2015;8:932-58.
[3] Denry I, Kelly JR. State of the art of zirconia for dental applications. Dent Mater. 2008;24:299-307.
[4] Bosshardt DD, Chappuis V, Buser D. Osseointegration of titanium, titanium alloy and zirconia dental implants: current knowledge and open questions. Periodontol 2000. 2017;73:22-40.

[5] Pieralli S, Kohal RJ, Lopez Hernandez E, Doerken S, Spies BC. Osseointegration of zirconia dental implants in animal investigations: A systematic review and meta-analysis. Dent Mater. 2018;34:171-82.

[6] Pieralli S, Kohal RJ, Jung RE, Vach K, Spies BC. Clinical Outcomes of Zirconia Dental Implants: A Systematic Review. J Dent Res. 2017;96:38-46.

[7] Degidi M, Artese L, Scarano A, Perrotti V, Gehrke P, Piattelli A. Inflammatory infiltrate, microvessel density, nitric oxide synthase expression, vascular endothelial growth factor expression, and proliferative activity in peri-implant soft tissues around titanium and zirconium oxide healing caps. J Periodontol. 2006;77:73-80.

[8] Roehling S, Astasov-Frauenhoffer M, Hauser-Gerspach I, Braissant O, Woelfler H, Waltimo T, et al. In Vitro Biofilm Formation on Titanium and Zirconia Implant Surfaces. J Periodontol. 2017;88:298-307.

[9] Welander M, Abrahamsson I, Berglundh T. The mucosal barrier at implant abutments of different materials. Clin Oral Implants Res. 2008;19:635-41.

[10] Hashim D, Cionca N, Courvoisier DS, Mombelli A. A systematic review of the clinical survival of zirconia implants. Clin Oral Investig. 2016;20:1403-17.

[11] Rodriguez AE, Monzavi M, Yokoyama CL, Nowzari H. Zirconia dental implants: A clinical and radiographic evaluation. J Esthet Restor Dent. 2018;30:538-44.

[12] Roehling S, Schlegel KA, Woelfler H, Gahlert M. Performance and outcome of zirconia dental implants in clinical studies: A meta-analysis. Clin Oral Implants Res. 2018;29 Suppl 16:135-53.

[13] Jung RE, Zembic A, Pjetursson BE, Zwahlen M, Thoma DS. Systematic review of the survival rate and the incidence of biological, technical, and aesthetic complications of single crowns on implants reported in longitudinal studies with a mean follow-up of 5 years. Clin Oral Implants Res. 2012;23 Suppl 6:2-21.

[14] Sivaraman K, Chopra A, Narayan AI, Balakrishnan D. Is zirconia a viable alternative to titanium for oral implant? A critical review. Journal of Prosthodontic Research. 2018;62:121-33.

[15] Scherrer SS, Mekki M, Crottaz C, Gahlert M, Romelli E, Marger L, et al. Translational research on clinically failed zirconia implants. Dent Mater. 2019;35:368-88.

[16] Monzavi M, Zhang F, Meille S, Douillard T, Adrien J, Noumbissi S, et al. Influence of artificial aging on mechanical properties of commercially and non-commercially available zirconia dental implants. J Mech Behav Biomed Mater. 2020;101:103423.

[17] Quinn G. A NIST recommended practice guide: fractrography of ceramics and glasses: Washington, DC: National Institute of Standards and Technology; 2016.

[18] Scherrer SS, Lohbauer U, Della Bona A, Vichi A, Tholey MJ, Kelly JR, et al. ADM guidance—Ceramics: guidance to the use of fractography in failure analysis of brittle materials. Dent Mater. 2017;33:599-620.

[19] Kelly JR, Campbell SD, Bowen HK. Fracture-surface analysis of dental ceramics. J Prosthet Dent. 1989;62:536-41.

[20] Kelly JR, Giordano R, Pober R, Cima MJ. Fracture surface analysis of dental ceramics: clinically failed restorations. Int J Prosthodont. 1990;3:430-40.

[21] Quinn JB, Quinn GD, Kelly JR, Scherrer SS. Fractographic analyses of three ceramic whole crown restoration failures. Dent Mater. 2005;21:920-9.

[22] Gahlert M, Burtscher D, Grunert I, Kniha H, Steinhauser E. Failure analysis of fractured dental zirconia implants. Clin Oral Implants Res. 2012;23:287-93.

[23] Scherrer SS, Quinn GD, Quinn JB. Fractographic failure analysis of a Procera AllCeram crown using stereo and scanning electron microscopy. Dent Mater. 2008;24:1107-13.

[24] Jodha KS, Salazar Marocho SM, Scherrer SS, Griggs JA. Fractal analysis at varying locations of clinically failed zirconia dental implants. Dent Mater. 2020;36:1052-8.

[25] Bethke A, Pieralli S, Kohal R-J, Burkhardt F, von Stein-Lausnitz M, Vach K, et al. Fracture Resistance of Zirconia Oral Implants In Vitro: A Systematic Review and Meta-Analysis. Materials (Basel). 2020;13:562.

[26] Jank S, Hochgatterer G. Success-rate of two-piece zirconia implants – a retrospective statistical analysis on 15,000 implants. Int J Oral Maxillofac Surg. 2015;44:e84.

[27] Spies BC, Fross A, Adolfsson E, Bagegni A, Doerken S, Kohal RJ. Stability and aging resistance of a zirconia oral implant using a carbon fiber-reinforced screw for implant-abutment connection. Dent Mater. 2018;34:1585-95.

[28] Zhang F, Meyer zur Heide C, Chevalier J, Vleugels J, Van Meerbeek B, Wesemann C, et al. Reliability of an injection-moulded two-piece zirconia implant with PEKK abutment after long-term thermo-mechanical loading. J Mech Behav Biomed Mater. 2020;110:103967.

[29] Monzavi M, Zhang F, Douillard T, Gremillard L, Noumbissi S, Nowzari H, et al. Microstructural analyses of artificial ageing in 5 commercially and non-commercially available Zirconia dental implants. J Eur Ceram Soc. 2020;40:3642-55.

[30] Oliva X, Oliva JD, Oliva JD, Prasad HS, Rohrer MD. Osseointegration of Zirconia (Y-TZP) Dental Implants: A Histologic, Histomorphometric and Removal Torque Study in the Hip of Sheep. International Journal of Oral Implantology and Clinical Research. 2013;4:55-62.

[31] Monzavi M, Noumbissi S, Nowzari H. The Impact of In Vitro Accelerated Aging, Approximating 30 and 60 Years In Vivo, on Commercially Available Zirconia Dental Implants. Clin Implant Dent Relat Res. 2017;19:245-52.

[32] Zhang F, Meyer Zur Heide C, Chevalier J, Vleugels J, Van Meerbeek B, Wesemann C, et al. Reliability of an injection-moulded two-piece zirconia implant with PEKK abutment after long-term thermo-mechanical loading. J Mech Behav Biomed Mater. 2020;110:103967.

[33] Kammermeier A, Rosentritt M, Behr M, Schneider-Feyrer S, Preis V. In vitro performance of one- and two-piece zirconia implant systems for anterior application. J Dent. 2016;53:94-101.

[34] Spies BC, Nold J, Vach K, Kohal R-J. Two-piece zirconia oral implants withstand masticatory loads: An investigation in the artificial mouth. J Mech Behav Biomed Mater. 2016;53:1-10.

[35] Ritchie RO. Mechanisms of fatigue-crack propagation in ductile and brittle solids. International Journal of Fracture. 1999;100:55-83.

[36] Scherrer SS, Quinn JB, Quinn GD, Wiskott HWA. Fractographic ceramic failure analysis using the replica technique. Dental materials : official publication of the Academy of Dental Materials. 2007;23:1397-404.

[37] Inokoshi M, Zhang F, Vanmeensel K, De Munck J, Minakuchi S, Naert I, et al. Residual compressive surface stress increases the bending strength of dental zirconia. Dent Mater. 2017;33:e147-e54.

[38] Kosmac T, Oblak C, Jevnikar P, Funduk N, Marion L. Strength and reliability of surface treated Y-TZP dental ceramics. J Biomed Mater Res. 2000;53:304-13.

[39] Kosmač T, Oblak C, Jevnikar P, Funduk N, Marion L. The effect of surface grinding and sandblasting on flexural strength and reliability of Y-TZP zirconia ceramic. Dent Mater. 1999;15:426-33.

[40] Okada M, Taketa H, Torii Y, Irie M, Matsumoto T. Optimal sandblasting conditions for conventional-type yttria-stabilized tetragonal zirconia polycrystals. Dent Mater. 2019;35:169-75.

[41] Zhang X, Liang W, Jiang F, Wang Z, Zhao J, Zhou C, et al. Effects of air-abrasion pressure on mechanical and bonding properties of translucent zirconia. Clin Oral Investig. 2021;25:1979-88.

[42] Sulaiman TA, Abdulmajeed AA, Shahramian K, Lassila L. Effect of different treatments on the flexural strength of fully versus partially stabilized monolithic zirconia. J Prosthet Dent. 2017;118:216-20.

[43] AlMutairi R, AlNahedh H, Maawadh A, Elhejazi A. Effects of Different Air Particle Abrasion Protocols on the Biaxial Flexural Strength and Fractography of High/Ultra-Translucent Zirconia. Materials. 2022;15:244.

[44] Zhang Y, Lawn BR, Rekow ED, Thompson VP. Effect of sandblasting on the long-term performance of dental ceramics. Journal of Biomedical Materials Research Part B: Applied Biomaterials. 2004;71B:381-6.

[45] Zhang Y, Lawn BR, Malament KA, Van Thompson P, Rekow ED. Damage accumulation and fatigue life of particle-abraded ceramics. Int J Prosthodont. 2006;19:442-8.

[46] Han J, Zhang F, Van Meerbeek B, Vleugels J, Braem A, Castagne S. Laser surface texturing of zirconia-based ceramics for dental applications: A review. Materials Science and Engineering: C. 2021;123:112034.

[47] Roehling S, Woelfler H, Hicklin S, Kniha H, Gahlert M. A Retrospective Clinical Study with Regard to Survival and Success Rates of Zirconia Implants up to and after 7 Years of Loading. Clin Implant Dent Relat Res. 2016;18:545-58.

[48] Esteves Lima RP, Abreu LG, Belém FV, Pereira GHM, Brant RA, Costa FO. Is Implantoplasty Efficacious at Treating Peri-Implantitis? A Systematic Review and Meta-Analysis. J Oral Maxillofac Surg. 2021;79:2270-9.

[49] Romeo E, Lops D, Chiapasco M, Ghisolfi M, Vogel G. Therapy of peri-implantitis with resective surgery. A 3-year clinical trial on rough screw-shaped oral implants. Part II: radiographic outcome. Clin Oral Implants Res. 2007;18:179-87.

[50] Bianchini MA, Galarraga-Vinueza ME, Bedoya KA, Correa BB, de Souza Magini R, Schwarz F. Implantoplasty Enhancing Peri-implant Bone Stability Over a 3-Year Follow-up: A Case Series. Int J Periodontics Restorative Dent. 2020;40:e1-e8.

[51] Romeo E, Ghisolfi M, Murgolo N, Chiapasco M, Lops D, Vogel G. Therapy of peri-implantitis with resective surgery. A 3-year clinical trial on rough screw-shaped oral implants. Part I: clinical outcome. Clin Oral Implants Res. 2005;16:9-18.

[52] Esteves Lima RP, Abreu LG, Belém FV, Pereira GHdM, Brant RA, Costa FO. Is Implantoplasty Efficacious at Treating Peri-Implantitis? A Systematic Review and Meta-Analysis. Journal of Oral and Maxillofacial Surgery. 2021;79:2270-9.

[53] Kohal RJ, Wolkewitz M, Tsakona A. The effects of cyclic loading and preparation on the fracture strength of zirconium-dioxide implants: an in vitro investigation. Clin Oral Implants Res. 2011;22:808-14.

[54] Ravidà A, Siqueira R, Saleh I, Saleh MHA, Giannobile A, Wang HL. Lack of Clinical Benefit of Implantoplasty to Improve Implant Survival Rate. J Dent Res. 2020;99:1348-55.

[55] Andreiotelli M, Kohal RJ. Fracture strength of zirconia implants after artificial aging. Clin Implant Dent Relat Res. 2009;11:158-66.

[56] Zhang Y, Lawn BR. Fatigue sensitivity of Y-TZP to microscale sharp-contact flaws. J Biomed Mater Res B Appl Biomater. 2005;72:388-92.

[57] Wu AY-J, Hsu J-T, Chee W, Lin Y-T, Fuh L-J, Huang H-L. Biomechanical evaluation of one-piece and two-piece small-diameter dental implants: In-vitro experimental and three-dimensional finite element analyses. Journal of the Formosan Medical Association. 2016;115:794-800.

[58] Karl M, Scherg S, Grobecker-Karl T. Fracture of Reduced-Diameter Zirconia Dental Implants Following Repeated Insertion. Int J Oral Maxillofac Implants. 2017;32:971-5.

[59] Matsui K, Ohmichi N, Ohgai M, Enomoto N, Hojo J. Sintering Kinetics at Constant Rates of Heating: Effect of Al_2O_3 on the Initial Sintering Stage of Fine Zirconia Powder. J Am Ceram Soc. 2005;88:3346-52.

[60] Zhang F, Vanmeensel K, Inokoshi M, Batuk M, Hadermann J, Van Meerbeek B, et al. Critical influence of alumina content on the low temperature degradation of 2–3mol% yttria-stabilized TZP for dental restorations. J Eur Ceram Soc. 2015;35:741-50.

[61] Willems E, Turon-Vinas M, Camargo dos Santos B, Van Hooreweder B, Zhang F, Van Meerbeek B, et al. Additive manufacturing of zirconia ceramics by material jetting. J Eur Ceram Soc. 2021;41:5292-306.

Figure captions
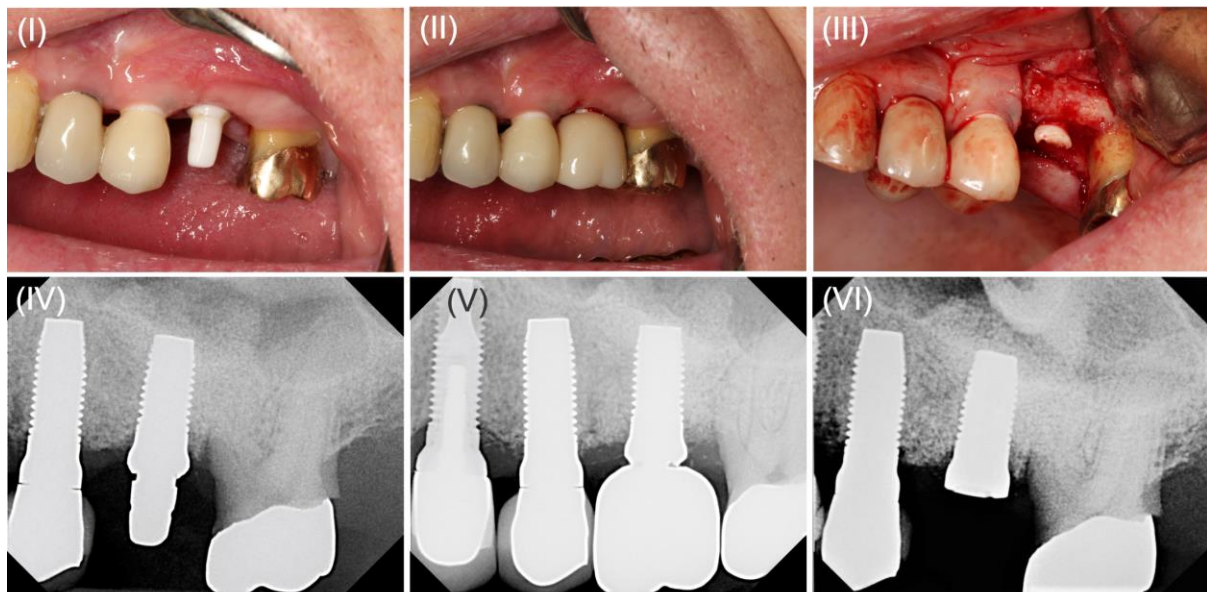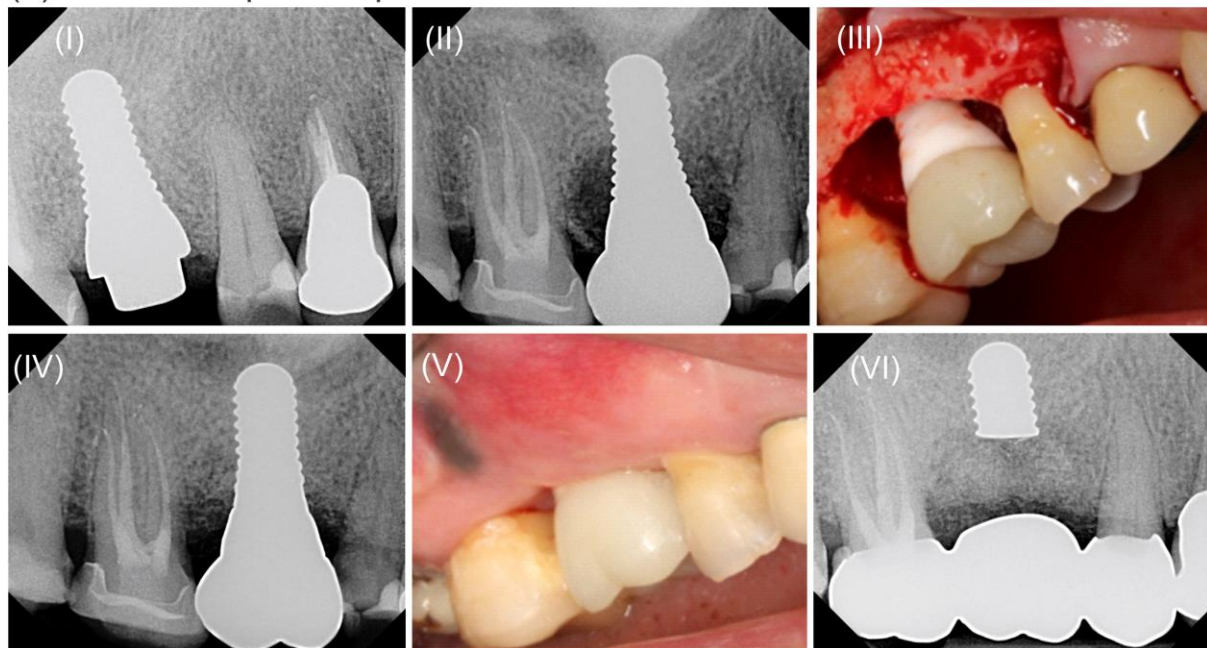
Fig. 1. Radiographic and clinical images of a Z-Systems 2p-45m implant and a CeraRoot 1p-3m implant. (a) Z-Systems 2p-45m implant: (I) Clinical images showing that the abutment and implant neck were heavily ground and prepared by the clinician prior to final restoration; (II) A disproportionately large crown was placed on the implant; (III) Surgical removal of the fractured implant. (IV) Radiograph taken prior to final restoration, demonstrating the grinding of the abutment and implant neck by the clinician; (V) Radiograph taken at the time of crown loosening due to fracture; (VI) Radiograph taken at the time of implant fracture (after 45 months of clinical service). (b) CeraRoot 1p-3m implant: (I) Five months following implant placement with the implant exposed and ready to be restored; (II) Peri-implantitis observed 2 years and 4 months following implant placement; (III) Osseous surgery and implantoplasty to treat the peri-implantitis; (IV) Periapical radiograph taken 1 month following osseous surgery;

(V) Clinical photo taken 1 month following osseous surgery; (VI) Implant fracture three months following osseous surgery.
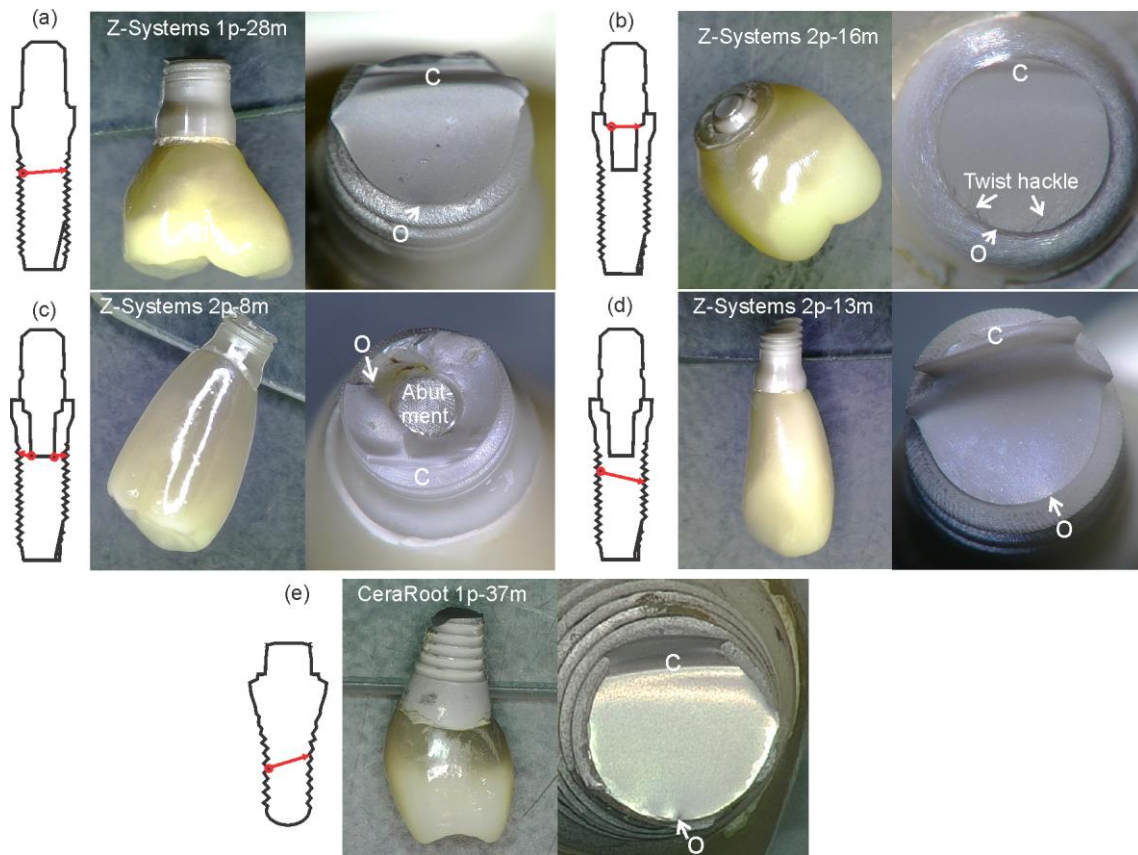
Fig. 2. Representative images of recovered crown-implant parts and fracture surfaces for the five different fractographic behaviors observed: (a) Z-Systems one-piece implant having failed at the endosseous part, i.e., CASE 1 with corresponding SEM shown in Fig. 3. (b) Z-Systems two-piece implant having failed at the abutment neck, i.e., CASE 2 with corresponding SEM shown in Fig. 4. (c) Z-Systems two-piece implant having failed at the inner surfaces of the abutment-implant connections with the abutment having been exposed, i.e., CASE 3 with corresponding SEM shown in Fig. 5. (d) Z-Systems two-piece implant having failed at the endosseous part/fixture, i.e., CASE 4 with corresponding SEM shown in Fig. 6. (e) CeraRoot one-piece implant having failed at the endosseous part, i.e., CASE 5 with corresponding SEM shown in Fig. 7. The compression curls and the fracture origins are marked by 'c' and an arrow and 'o', respectively. The red circle and arrow on the implant illustration show the fracture origin and the main crack-propagation direction.
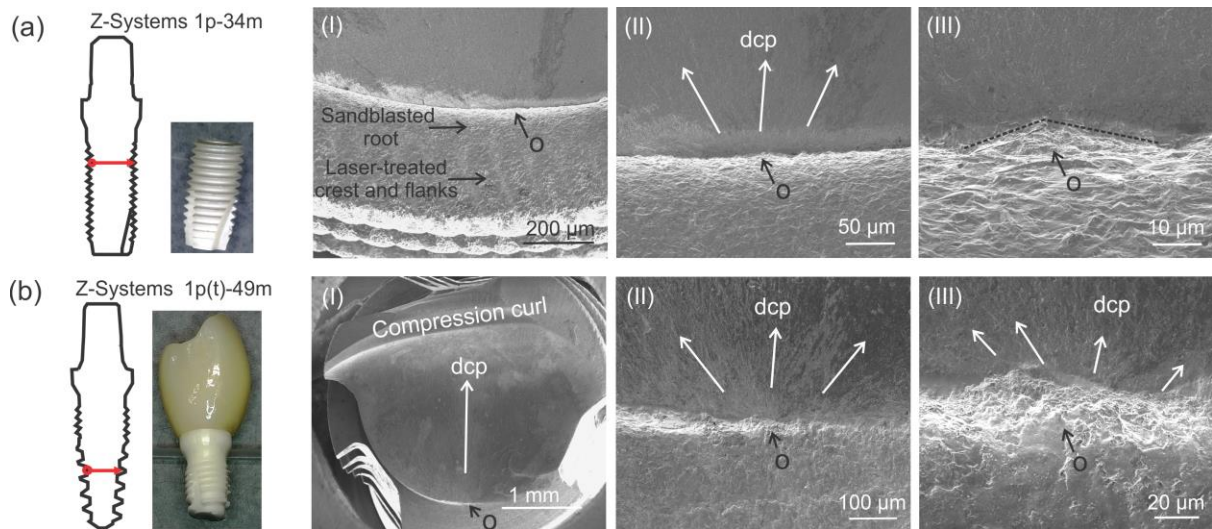
Fig. 3. Representative fracture surfaces of Z-Systems one-piece implants that failed at the endosseous part (CASE 1). (a) 1p-34m: (I) Overview of the fracture surface at low magnification; (II-III) Higher magnifications of the fracture surface showing the fracture origin. The implant external surface showed a v-notch shaped cut at the fracture origin (o). (b) Tapered 1p(t)-39m: (I) Overview of fracture surface at low magnification; (II-III) Higher magnifications showing the fracture origin. The implant surface showed deep cuts at origin (o). The direction of crack propagation (dcp) is indicated by white arrows.
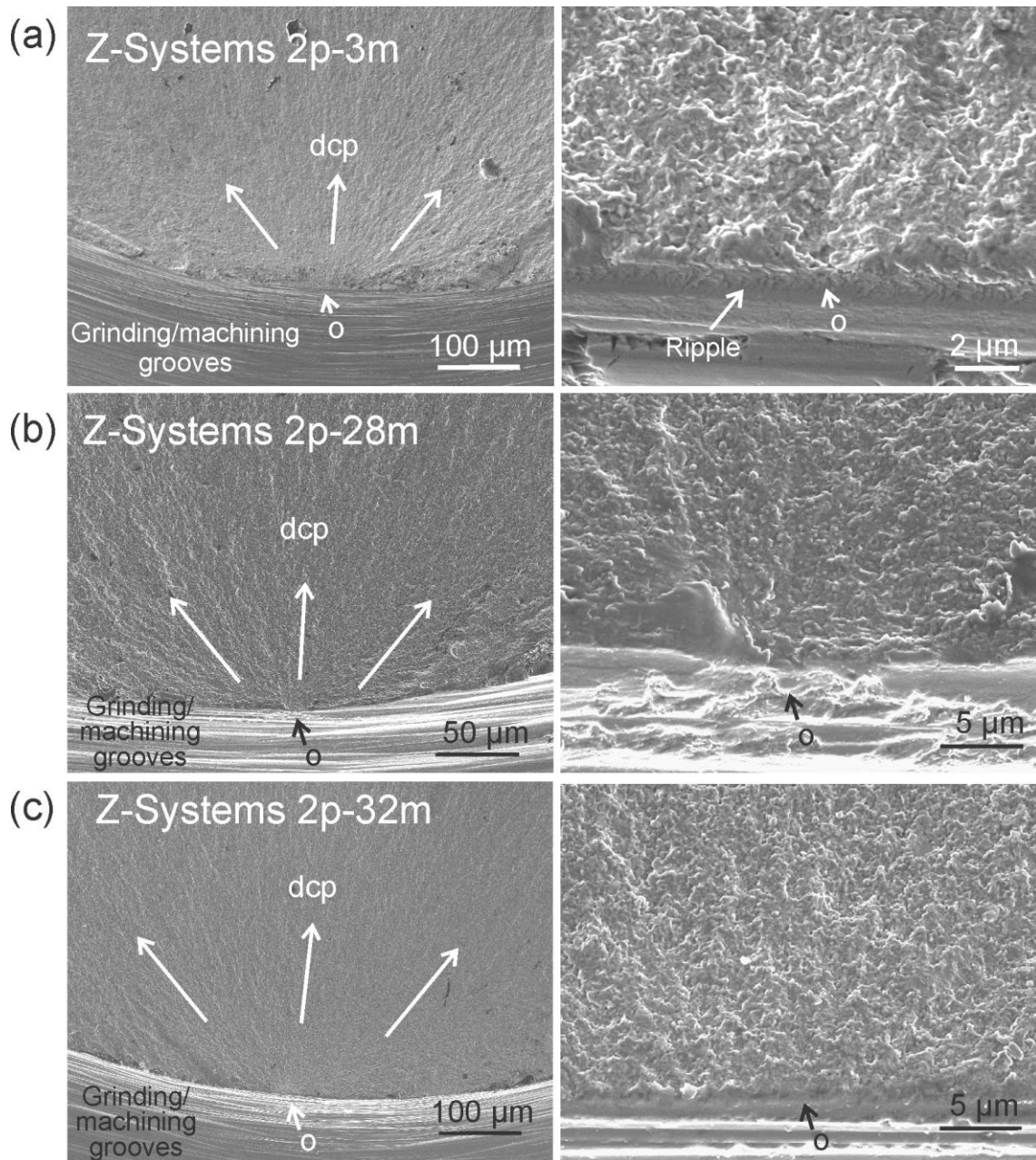
Fig. 4. Representative fracture surfaces of Z-Systems two-piece implants that failed at the abutment neck (CASE 2): (a) Z-Systems 2p-3m implant with the fracture origin connected to the ripple shaped grinding/machining scar; (b) Z-Systems 2p-3m implant with the fracture origin connected to the v-shaped deep cut; (c) Z-Systems 2p-32m implant, for which no clear defect was observed within the grinding/machining grooves that could be connected to the fracture origin. The direction of crack propagation (dcp) and the fracture origin (o) are indicated by arrows.
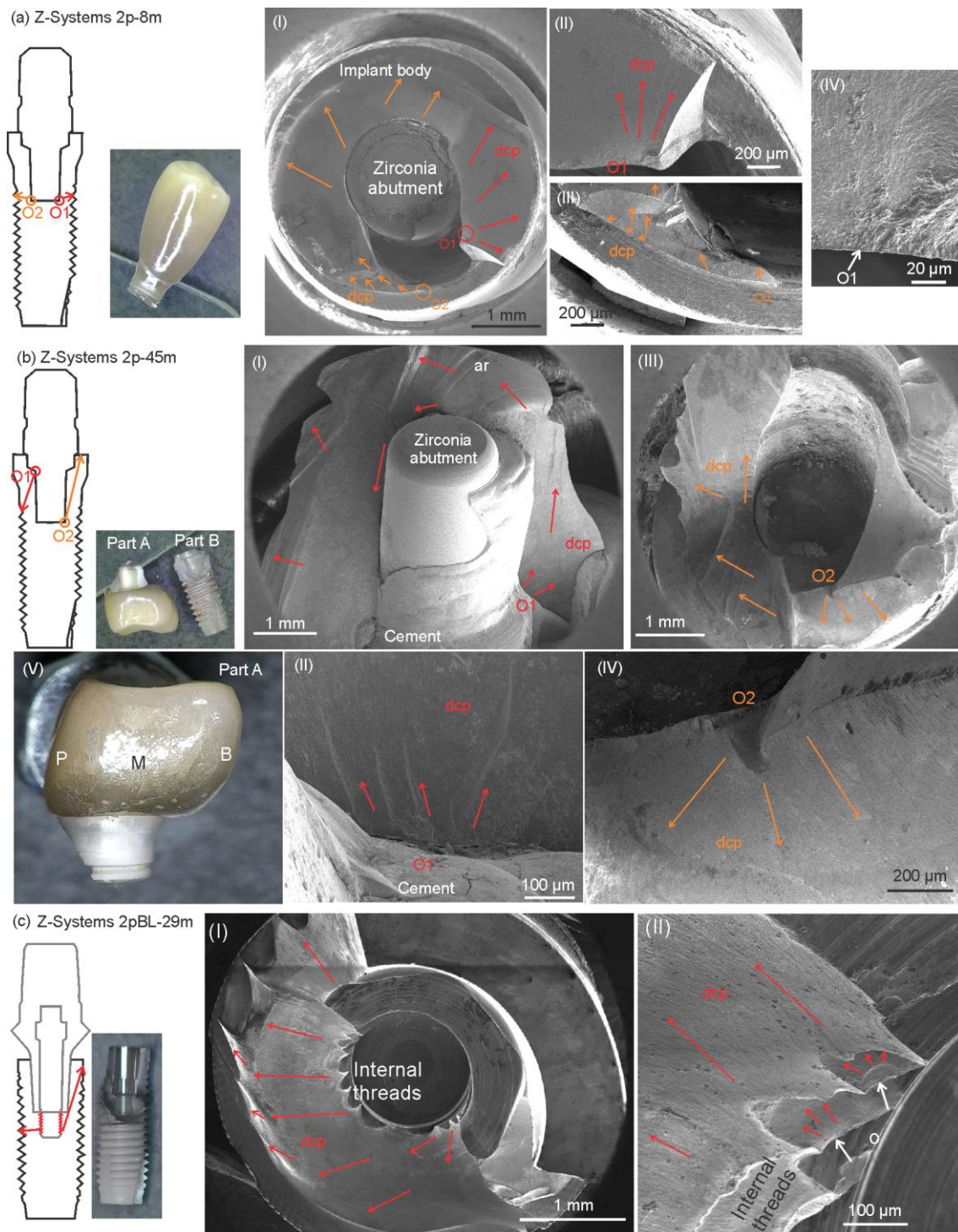
Fig. 5. Z-Systems two-piece implants with fracture-initiation sites observed at the inner surfaces at the abutment-implant connection (CASE 3). The crack-propagation direction (dcp) was marked with red and orange arrows, corresponding to the identified first fracture origin (O1) and second fracture origin (O2). Arrest lines (ar) were visualized for the Z-Systems 2p-45m implant. (a) Z-Systems 2p-8m two-piece cemented and self-tapping tissue-level implant. The upper part of the implant, the abutment and the crown were recovered. (b) Z-Systems 2p-45m two-piece cemented and self-tapping tissue-level implant. Two parts of the fractured implant were recovered. The fracture surface of part A was shown in I-II (red dcp); the fracture surface of part B was shown in III-IV (orange dcp). The central axis of this implant was off-centered due to the buccal extension, as can be seen in V. (c) Z-Systems 2pBL-29m two-piece

screw-retained bone-level implant. Only the zirconia implant was recovered (without screw and abutment).
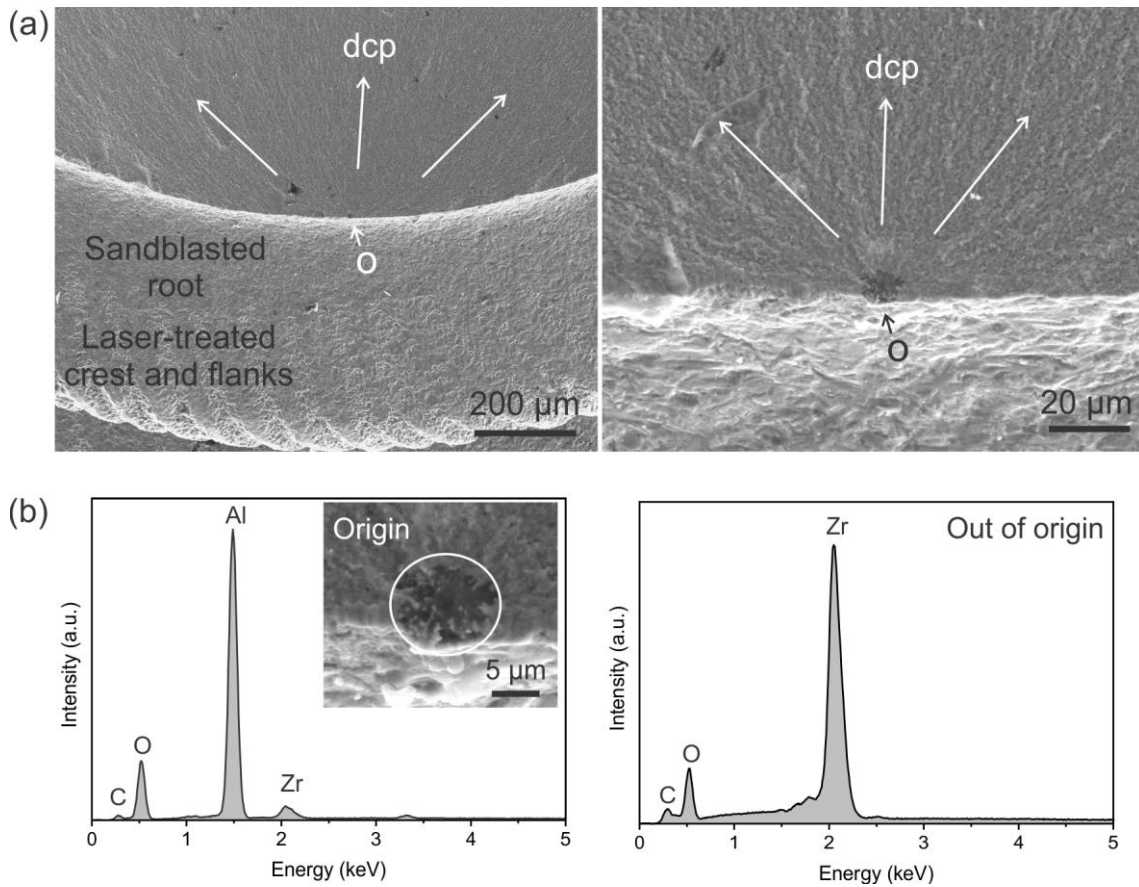
Fig. 6. Z-Systems 2p-13m two-piece implant with a fracture-initiation site observed at the external surface between two threads at the implant endosseous region (CASE 4): (a) Fracture surfaces; (b) EDS showing the elemental composition of a darker precipitate observed at the fracture origin (left) and of the lighter contrast area away from the fracture origin (right) for comparison.
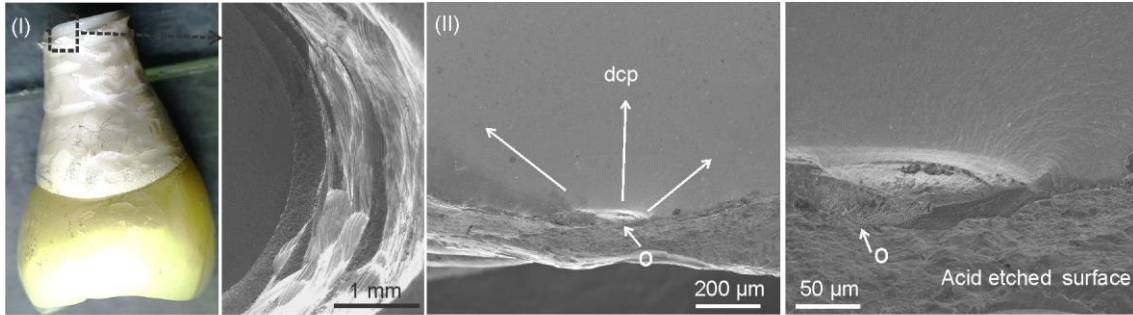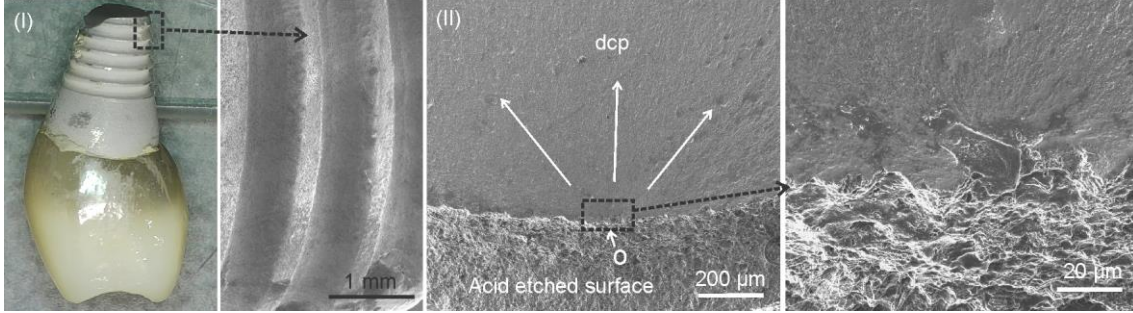
Fig. 7. CeraRoot one-piece implants with the fracture-initiation site observed at the external surface between two threads at the endosseous region (CASE 5). (a) CeraRoot 1p-3m: (I) Optical and SEM images showing the thread damages with many chips caused by implantoplasty; (II) Implant revealing a large chipping defect identified at the fracture-origin site (o), which was possibly related to surface implantoplasty; (b) CeraRoot 1p-37m: (I) Optical and SEM images showing the non-treated implant threads. (II) Implant without a critical defect having been observed at the fracture-origin area (o), as marked by the black square that is magnified in the right image.
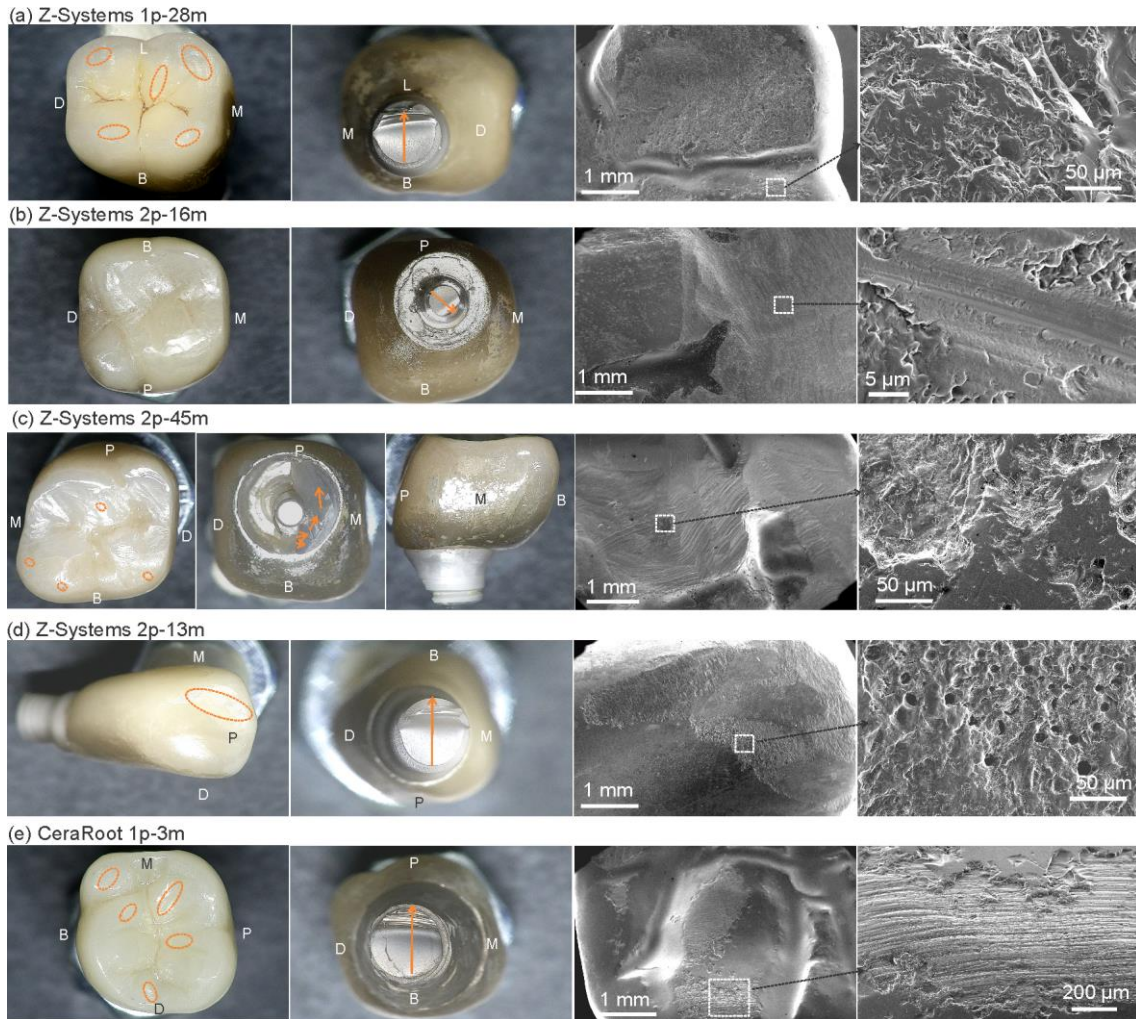
Fig. 8. The crown orientation (B = buccal, D = distal, M = mesial, P = palatal, L = lingual) and the crown-surface condition on the representative implants for each case. (a) Z-Systems 1p-28m from CASE 1. (b) Z-Systems 2p-16m from CASE 2. (c) Z-Systems 2p-45m from CASE 3. The buccal bulk extension makes the central axis of the implant off-centered. (d) Z-Systems 2p-13m from CASE 4. (e) CeraRoot 1p-3m from CASE 5. The orange arrow indicates the direction of crack propagation. The orange circles indicate the areas with occlusal contacts.

Tables

Table 1. Details of the studied implants.

Manufacturer	Materials and processing	Surface treatments	Type	Brand name and implant diameter (mm)	Implant label	Implant position	Time to failure (Months)
Z-Systems	3Y-TZP Isostatic pressing, sintering, hipping, grinding	Sandblasting, laser modification	One-piece (n=4)	Z5m (n=3, ∅ 4)	Z-System 1p-13m/28m/34m	Molar, premolar	13 Mo, 28 Mo, 34 Mo
				Z5m(t), tapered implants (n=1, ∅ 4)	Z-system 1p(t)-49m	Premolar	49 Mo
			Two-piece (n=10)	Z5c (n=9, ∅ 5/4)	Z-system 2p-3m/8m/13m/16m/28m/29m/30m/32m/45m	Molar, premolar, incisor	3 Mo, 8 Mo, 13 Mo, 16 Mo, 28 Mo, 29 Mo, 30 Mo, 32 Mo, 45 Mo
				Z5-BL, bone-level implant (n=1, ∅ 4)	Z-system 2pBL-29m	Canine	29 Mo
CeraRoot	3Y-TZP Injection molding, sintering	Acid etching	One-piece (n=2)	CeraRoot 16 (n=1, ∅ 5)	CeraRoot 1p-3m/37m	Molar	3 Mo, 37 Mo

Table 2. Five different fracture modes observed for recovered implants.

Manufacturer	Z-Systems (CASE 1-4)				CeraRoot (CASE 5)
	1	**2**	**3**	**4**	**5**
Cases	**One-piece implant failed at the endosseous part (n=5)**	**Two-piece implant failed at the abutment (n=6)**	**Two-piece implant failed at the abutment-implant connection with abutment exposure (n=3)**	**Two-piece implant failed at the endosseous part without abutment exposure (n=1)**	**One-piece implant failed at the endosseous part (n=2)**
Samples	Z-Systems 1p-13m/28m/34m/49m Z-Systems 1pt-49m (∅ 4 mm)	Z-Systems 2p-3m/16m/28m/29m/30m/32m (∅ 5 mm)	Z-Systems 2p-8m/45m Z-Systems 2pBL-29m (∅ 5/4 mm)	Z-Systems 2p-13m (∅ 4 mm)	CeraRoot 1p-3m/37m (∅ 5 mm)

Supplementary documents
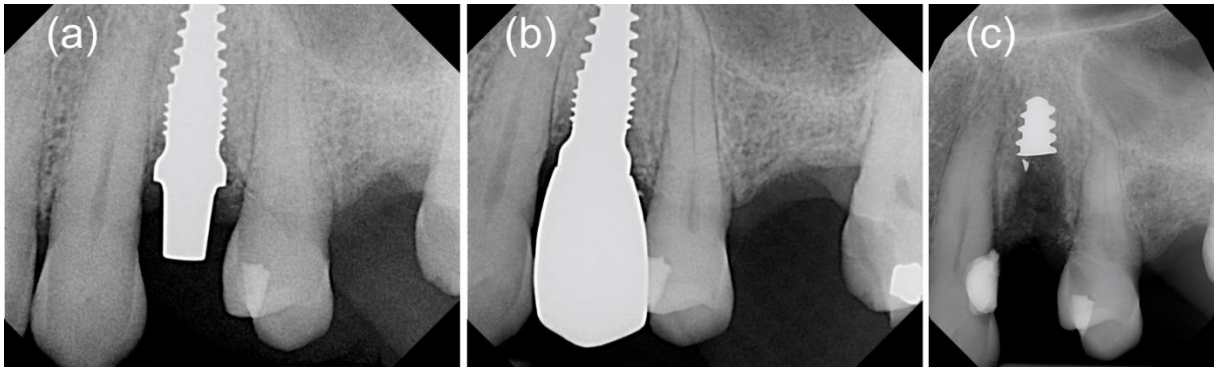
Fig. S1. Radiographic images of a tapered one-piece Z-Systems implant (1pt-49m): (a) Implant placed; (b) Implant with solitary crown; (c) Implant fracture after 49 months of clinical service.
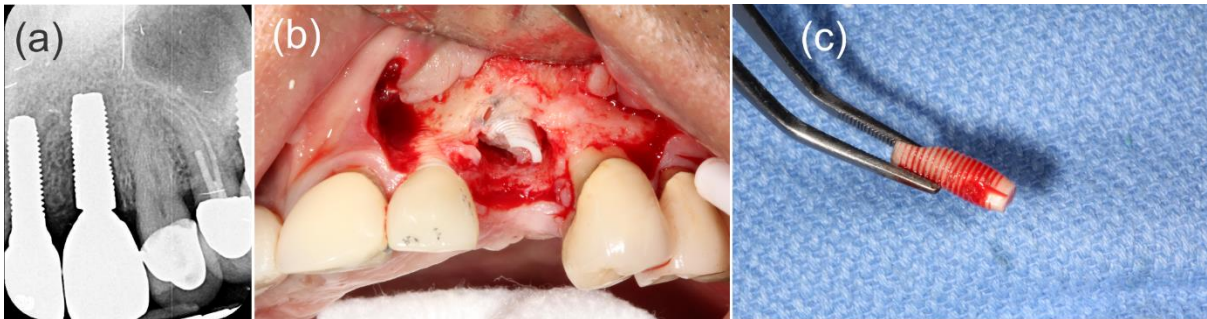
Fig. S2. Radiographic and clinical images of a fractured Z-Systems 2pBL-29m implant and its removal (a-c).
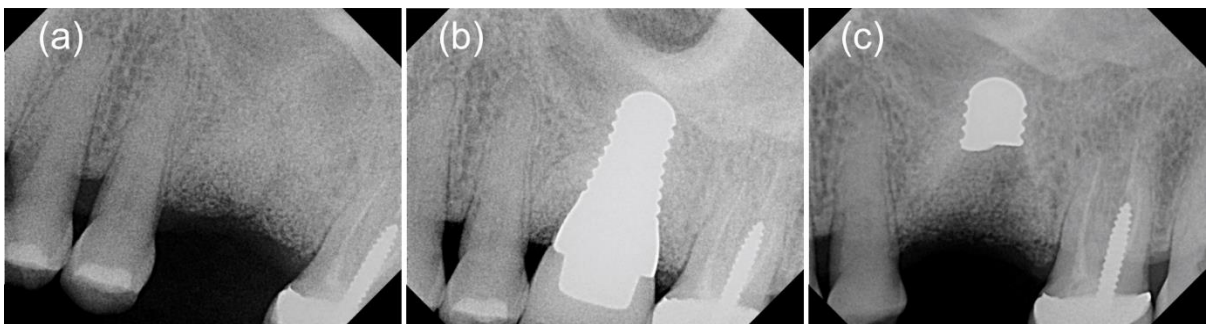
Fig. S3. Radiographic images of a CeraRoot 1p-37m implant (a-c): (a) Periapical radiograph prior to implant placement; (b) Periapical radiograph at final restoration; (c) Periapical.
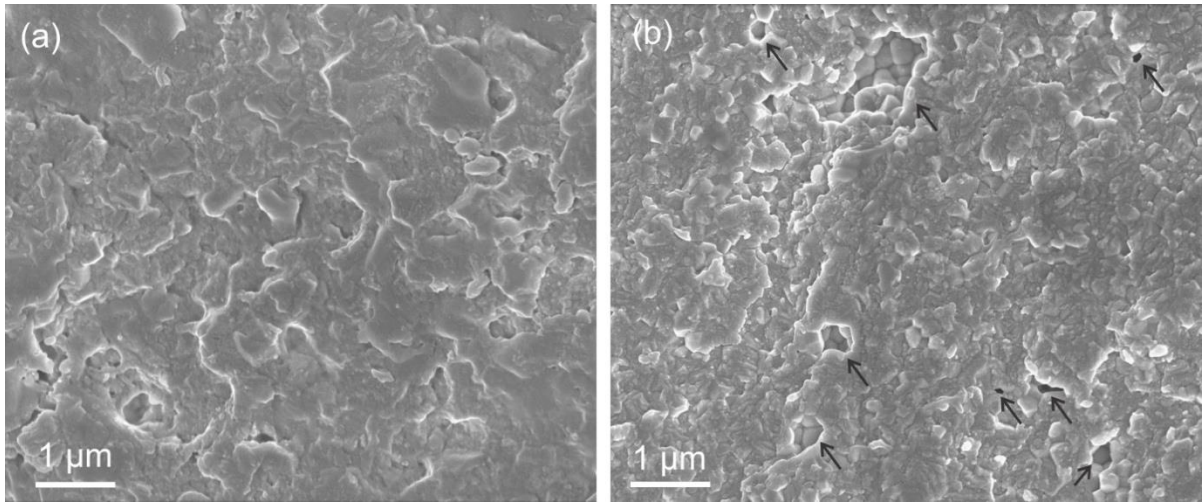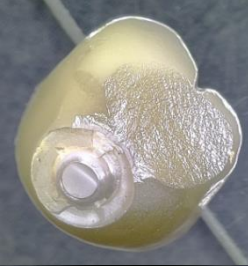
Fig. S4. Fracture of zirconia grains for a Z-Systems implant in (a) and a CeraRoot implant in (b).

Supplementary table

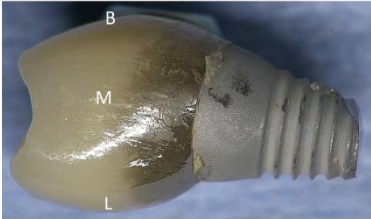**Table S1**. Clinically failed zirconia implants studied in this work.

Implant label	Type	Diameter (mm)	Implant location by tooth position	Time to failure	Additional optical images	Additional marks for the clinical and treatment planning implications
CASE 1: Z-Systems one-piece implant having failed at the endosseous part						
Z-Systems 1p-13m	One-piece Z5m	4	Mandibular first molar	05-12-2018 to 24-01-2020 1 Yr + 1 Mo		-
Z-Systems 1p-28m		4	Mandibular first molar	21-02-2017 to 23-06-2019 2 Yr + 4 Mo		Narrow diameter implant placed in the mandibular first molar position.
Z-Systems 1p-34m		4	Mandibular first premolar	19-03-2017 to 19-01-2020 2 Yr + 10 Mo		-
Z-Systems 1pt-49m	One-piece Z5m(t)	4	Maxillary first premolar	05-03-2017 to 27-04-2021 4 Yr + 1 Mo		Deep insertion with the restoration margin 3 mm below the alveolar crest; large crown to compensate for the deep placement of the implant; multiple posterior teeth missing.

CASE 2: Z-Systems two-piece implant having failed at the abutment neck					
Z-Systems 2p-3m		5	Maxillary first molar	19-04-2019 to 19-07-2019 3 Mo		Surface of the abutment and shoulder of the implant ground and prepared prior to restoration.
Z-Systems 2p-16m		5	Maxillary first Molar	12-01-2018 to 23-05-2019 1 Yr + 4 Mo		Surface of the abutment and shoulder of the implant ground and prepared prior to restoration.
Z-Systems 2p-28m	Two-piece Z5c	5	Maxillary first molar	28-04-2017 to 20-08-2019 2 Yr + 4 Mo		Deep insertion with the restoration margin 2 mm below the alveolar crest; surface of the abutment and shoulder of the implant ground and prepared prior to restoration.
Z-Systems 2p-29m		5	Maxillary first molar	06-10-2016 to 29-03-2019 2 Yr + 5 Mo		Surface of the abutment and shoulder of the implant ground and prepared prior to restoration.

Z-Systems 2p-30m		5	Maxillary first molar	19-10-2016 to 10-04-2019 2 Yr + 6 Mo		Surface of the abutment and shoulder of the implant ground and prepared prior to restoration.
Z-Systems 2p-32m		5	Maxillary first premolar	06-12-2016 to 01-08-2019 2 Yr + 8 Mo		Surface of the abutment and shoulder of the implant ground and prepared prior to restoration.
CASE 3: Z-Systems two-piece implant having failed at the abutment-implant connection with the abutment exposed						
Z-Systems 2p-8m	Two-piece Z5c	4	Premolar	01-11-2019 to 09-28-2019 8 Mo		Position with the restoration margin 3 mm below the alveolar crest; disproportionately large crown.
Z-Systems 2p-45m	Two-piece Z5c	5	Maxillary first molar	03-04-2017 to 11-01-2021 3 Yr + 9 Mo		Disproportionately large crown to compensate for the large mesial and distal space in relation to the implant; positioning of this implant was too much above the gingiva, which was not esthetic by exposing the white zirconia implant; the clinician re-prepared the implant and the abutment by grinding the implant and abutment neck in order to get the shoulder at the level of the gum.

Z-Systems 2pBL-29m	Two-piece Z5-BL	4	Canine	15-02-2019 to 28-07-21 2 Yr + 5 Mo		-

CASE 4: Z-Systems two-piece implant having failed at the implant endosseous part without abutment exposure

Z-Systems 2p-13m	Two-piece Z5c	4	Lateral incisor	03-12-2018 to 24-01-2020 1 Yr + 1 Mo		Non-optimal prosthetic position with the restoration margin 3 mm below the alveolar crest; disproportionately large crown; implant was positioned too buccally.

CASE 5: CeraRoot one-piece implant having failed at the implant endosseous part

CeraRoot 1p-3m	One-piece	4.8 (apical area), 6.5 (most coronal threaded part)	Maxilllary first molar	Placed on 20-8-2016; Osseous surgery and implantoplasty on the implant surface on 17-04-2019; Fractured on 29-07-2019 3 Mo		Peri-implantitis treated with implantoplasty of the implant surface with bone graft and guided tissue regeneration.
CeraRoot 1p-37m		4.8 (apical area), 6.5 most coronal threaded part)	Maxillary first Molar	20-03-2018 to 29-04-2021 3 Yr + 1 Mo		Implant inserted in a previously heavily grafted site.